

# Developing a Benzimidazole Silica-Based Hybrid Sol-gel Coating with Significant Corrosion Protection on Aluminum Alloys 2024-T3 †

Magdi H. Mussa<sup>1,2\*</sup>, F. Deeba Zahoor<sup>3,4</sup>, Oliver Lewis<sup>3</sup>, and Nicholas Farmilo<sup>3,5</sup>

<sup>1</sup> Mechanical and Energy Department, The Libyan Academy for Graduate study, Tripoli, Libya; magdimosa1976@gmail.com (MM)

<sup>2</sup> Mechanical Engineering Department, Sok Alkhamis Imsehel High Tec. Institute, Tripoli, Libya ; magdimosa1976@gmail.com (MM)

<sup>3</sup> Materials and engineering Research institute MERI, Sheffield Hallam University, Howard Street, Sheffield, UK ; O.Lewis@shu.ac.uk (OL), F.Zahoor@sheffield.ac.uk (DF), nfarmilo@gmail.com (NF)

<sup>4</sup> Department of Chemistry, University of Sheffield, Sheffield, UK ; F.Zahoor@sheffield.ac.uk (DF)

<sup>5</sup> Tideswell Business Development Ltd, Ravensfield Sherwood Rd, Buxton, UK ; nfarmilo@gmail.com (NF)

\* Correspondence: magdimosa1976@gmail.com; Tel.: +447404496955

† 2nd International Electronic Conference on Applied Sciences, Applied Physics, 15 - 31/10/2021.

**Citation:** Mussa, M. H. ; Zahoor , D. F.; Lewis , O. and Farmilo , N., "Developing a Benzimidazole Silica-Based Hybrid Sol-gel Coating with Significant Corrosion Protection on Aluminum Alloys 2024-T3". *AP Proceedings* **2021**, *68*, x. <https://doi.org/10.3390/xxxxx>

Published: date

**Publisher's Note:** MDPI stays neutral with regard to jurisdictional claims in published maps and institutional affiliations.



**Copyright:** © 2021 by the authors. Submitted for possible open access publication under the terms and conditions of the Creative Commons Attribution (CC BY) license (<http://creativecommons.org/licenses/by/4.0/>).

**Abstract:** The inherent reactivity of the Al-Cu-Mg alloys is such that their use for building structural, maritime, and aeroplane components with great strength/weight ratio, it would not be possible without good anti-corrosion systems. These systems could be considered as imitations of the protection mechanism found with the conventional hexavalent chromium-based system, but also limiting the environmental impact, precisely without toxic or carcinogenic effect, and should also be eco-friendly. Silica-based hybrid protective coatings have been shown to exhibit excellent chemical stability combined with the ability to reduce the corrosion of metal substrates. However, research shows that sol-gel has some limitations in terms of the period of anti-corrosive properties. Therefore, this work reports the performance of a silica-based hybrid sol-gel coating encapsulated with Benzimidazole (BZI) that can be applied to light alloys to form a crack-free coating. This coating was applied on AA 2024-T3 and cured at 80°C. The high corrosion resistance performance results from the combination of good adhesion, the hydrophobic property of the silica-based hybrid coating and the presence of the encapsulated (BZI) film-forming volatile corrosion inhibitor, which will be released at pores within the coating system resulting in film-forming, reducing the cathodic reaction at cathodic sites. The evaluation of this mechanism is based upon using electrochemical testing techniques. The anti-corrosion properties of the coatings were studied immersed within 3.5% NaCl by using electrochemical impedance spectroscopy (EIS) and Potential-dynamic polarization scanning (PDPS). The chemical confirmation was done by infrared spectroscopy (ATR-FTIR), supported by analyzing the morphology of the surface before and after the immersion testing by using scanning electron microscopy (SEM). The Benzimidazole-silica-based hybrid coating exhibited excellent anti-corrosion properties, providing an adherent protection film on the aluminium alloy 2024-T3 samples compared to sol-gel-only and bare material, with cost-effective and as an eco-friendly system.

**Keywords:** Silica-based hybrid sol-gel coating, electrochemical testing, corrosion protection, aluminium alloys.

## 1. Introduction

Silica-based hybrid protective coatings using sol-gel technology have shown exceptional ability to reduce corrosion on the metal surface combined with high chemical stability. However, the sol-gel technique only has some limitations in terms of barrier anti-corrosive properties. By using the encapsulated corrosion inhibitors, will enhance the corrosion protection of sol-gel systems. The development of corrosion inhibitors compounds

has created many effective inhibitors with heterocyclic organic functional groups consisting of oxygen, nitrogen, phosphorus and sulphur attached as heteroatoms [1], [2].

Benzimidazole (BZI) is identified as a low pH film-forming corrosion inhibitor used for copper and steel with a heterocyclic aromatic organic compound structure. That could be used as both an effective volatile or injectable corrosion inhibitor with other soluble carriers as it has the chemical structure that contains both a benzene group and the active group imidazole, which can be used in the oil and gas industry by using inhibitors injection pumps [3]. BZI structure is shown in figure 1.1.

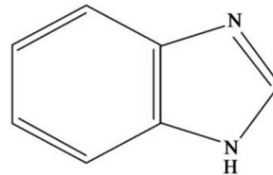


Figure 1.1 chemical structure of the Benzimidazole (BZI)

The great thing is that BZI is available commercially with cost-effectiveness as a raw material for many applications. Of course, the primary use is in pharmaceutical applications to use as a fungicide [4]. However, applied engineering was involving this kind of material and its derivatives in many applications. For instance, Antonijevic 2009 et al. [2] mentioned it as an inhibitor that demonstrated excellent inhibition of corrosion to protect carbon steel pipeline in corrosive acidic media of hydrochloride solution [2], [5].

The mechanism of inhibition by BZI or its derivatives on metal, which were studied especially on copper and steel [5]–[7], found that the BZI and its derivatives may be seen positioned in a parallel adsorption arrangement. As a result, there was a close joining with the surface crating thin film [5], [6]. The rearrangement and adsorption of BZI in this position are due to the donation of Pi electron ( $\pi$  electron) and the one pair of electrons on the nitrogen atoms, compensating the benzimidazole molecules to the iron atoms or copper that unoccupied D-orbital. These interactions explain the strong adsorption connection to the surface, and as a result, it will protect the mild steel from direct corrosion [5], [6], despite some mention of using BZI derivatives in some studies and patents, J. Colreavy et al. and S. Vijaykumar et al. mentioned in their patents to use the same family of these inhibitors sol-gel technique on steel or other metals as a limitation of the use only. The truth is there have been no real studies to combine BZI, or its derivatives, with the silicate sol-gel coating technique to use as a corrosion inhibitor on aluminium alloy AA2024-T3 [8], [9].

## 2. EXPERIMENTAL WORK

### 2.1. Sol-Gel Preparation

in this study, the used hybrid silica-based sol-gel was synthesized from tetraethyl orthosilicate silane (TEOS) and trimethoxymethylsilane (MTMS) purchased from Sigma-Aldrich. The precursors mixed in isopropyl alcohol by adding dropwise deionized (DI) water in the molar ratio of 18: 14: 17: 220, respectively, until the hydrolyzing and condensation reactions. The silica-based sol-gel mixture was then enhanced by adding poly-siloxane (PSES) solution, as mentioned in the previous work [10]. This formula was used as the baseline coating and labelled SHX-80. The benzimidazole modified hybrid silica-based sol-gel is labelled as BZI-SHX-80. It was prepared by encapsulating 3.5 vol.% of solution 1:1 of ethanol and benzimidazole (BZI) purchased from Sigma-Aldrich into the unmodified SHX-80 by wise dropping and stirring. The formulation was then left for 24 hours.

## 2.2 Substrate Preparation and Film Deposition

The commercially aluminium alloy AA2024-T3 Q-panels made with dimensions of (102 mm × 25 mm × 1.6 mm) were purchased from Q-Lab for use as test substrates [11]. First, the received Q-panels were washed with a commercial aluminium base surfactant cleaner and then rinsed with DI water. After that, rewashed with acetone to remove organic residues on the surface. Then spray the sol-gel to the pre-cleaned aluminium alloy substrates. The distance from the spraying gun to the surface was approximately 150 mm. Over three passes, the coating was built up to keep the thickness standard for all samples about 15 μm ±2. After that, the coated samples were left in the air for 10 min before being annealed at 80° C for 4 hours. Table 1 shows experiment codes used to identify samples.

**Table 1.** sample identification table

No.	Identifier	Formula Base Composite	(BZI) v/v%	Curing Temperature
1-	SHX-80	TEOS+MTMS+PSX	-	80°C
2-	ZBI-SHX-80	TEOS+MTMS+PSX	3.5%	80°C
3-	Bare AA2024 T3	-	-	-

## 2.3 Coating Testing and Characterization

Electrochemical tests were performed on the coatings to assess their corrosion resistance. Tests were conducted by using a Princeton Applied Research PARSTAT 2273. The corrosion performance of the sol-gel coated and uncoated aluminium alloy was evaluated using electrochemical impedance spectroscopy (EIS) and potentiodynamic polarization (PDPS) scans. With a tested area of 1.00 mm<sup>2</sup> in the centre of the samples in aerated 3.5% NaCl. The tests were carried at room temperature (20° C +/- 2° C). Prior to polarisation, the electrode potential was monitored for approximately 1 hour in electrolyte solution until stability. The sample was polarised with PDPS at a scan rate of 1.667 mVs<sup>-1</sup> from the initial potential of -250 mV vs OCP to +750 mV vs SCE. The electrochemical impedance measurements were recorded between 100 kHz to 10 MHz with a sinusoidal AC RMS value of 10 mV [12].

## 3. Results and discussion

### 3.1 ATR-FTIR for BZI-SBX-80 sol-gel chemical composition

The organic BZI was successfully incorporated into the SHX sol-gel by comparing the infrared spectrum obtained from the BZI-SHX-80 coating to the unmodified SHX-80. This is enlarged in figure 3.1. In the spectrum of the BZI-modified coating, several peaks are seen relating to the BZI molecule. These peaks can be observed and remain in the BZI-SBX-80 sol-gel coated sample. They are as follows: weak imine C=N stretching presents at 1564.5 cm<sup>-1</sup>, and carbon double bond C=C stretching peaks at about 1477 cm<sup>-1</sup>, 1458 cm<sup>-1</sup> and 1408 cm<sup>-1</sup>, respectively. Similarly, the fingerprint of the aromatic amines stretching C-N can be detected at 1364 and 1300 cm<sup>-1</sup>, respectively, which can be used to confirm the benzimidazole presence in the sol-gel formula. The C-H out-of-plane bending is characterized by peaks in 768 and 745 cm<sup>-1</sup>[13].



$5.98 \times 10^{-10} \text{A/cm}^2$  for (BZI-SHX-80) and  $1.1 \times 10^{-9} \text{A/cm}^2$  for (SHX-80) respectively, and as compared to  $7.1 \times 10^{-6} \text{A/cm}^2$  of the bare AA2024-T3 alloy. The shift in  $E_{\text{corr}}$  indicates that the anodic is inhibited to a greater degree than the cathode in BZI -SHX 80 sol-gel mixture. This could be attributed to the benzimidazole nitrogen active atoms bridging to the substrate surface [5], [6].

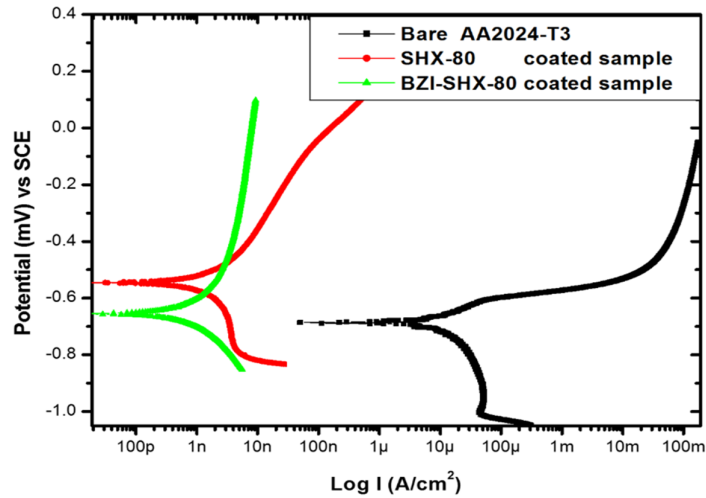


Figure 3.3, (PDPs) Polarization curves for the bare and sol-gel coated samples with different organic inhibitors in 3.5% NaCl

### 3.4 Electrochemical Impedance Spectroscopy (EIS)

#### 3.4.1 Impedance magnitude Bode plots

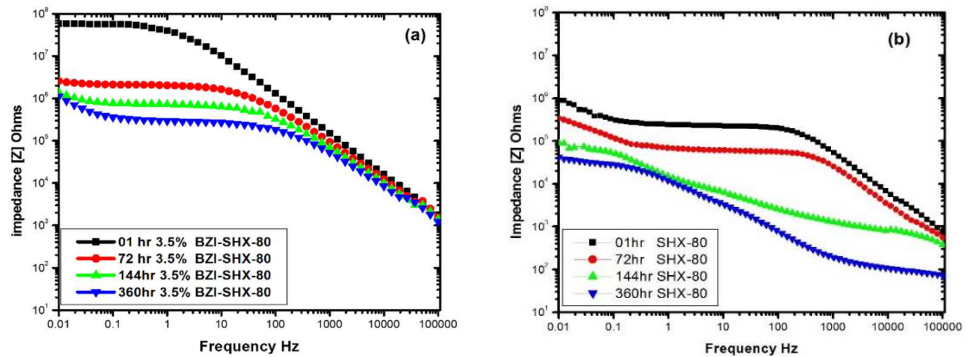


Figure 3.4, Impedance magnitude Bode plots for (a) BZI-SHX-80 and (b) SHX-80.

As it is shown in Figure 3.4, after the first hour of immersion, the overall impedance of BZI-SHX-80 at low frequencies was increased by approximately two orders of magnitude to SHX-80 coated samples, with values of  $5.7 \times 10^7 \text{ ohms.cm}^{-2}$  (BZI-SHX-80), compared to  $9.1 \times 10^5 \text{ ohms.cm}^{-2}$  (SHX-80). After 360 hours, the BZI-SHX-80 coated samples dropped about one and a half orders of magnitude; this could be due to the electrolyte diffusion and expansion of the pores in the coating matrix. However, this drop is not affecting the generally visible protection in the electrolyte, suggesting the film of BZI has been created on the metal surface [10]. A noticeable measured impedance was observed to the SHX-80 coated sample at about  $3.4 \times 10^4 \text{ ohms.cm}^{-2}$  after 360 hrs. This might be attributable to the coating resistance beginning to reduce due to the creation of rounded pitting under the coatings. Also, The high frequencies impedance fall of about one of magnitude; this impedance is considered higher than SBX-80 coating in the middle-frequency range between  $10^5$  to  $10^6 \text{ Hz}$ . It may be attributed to the coating pores and cracking that occurred.

3.4.2 Using Nyquist plots for Investigating the corrosion protection behaviour

2

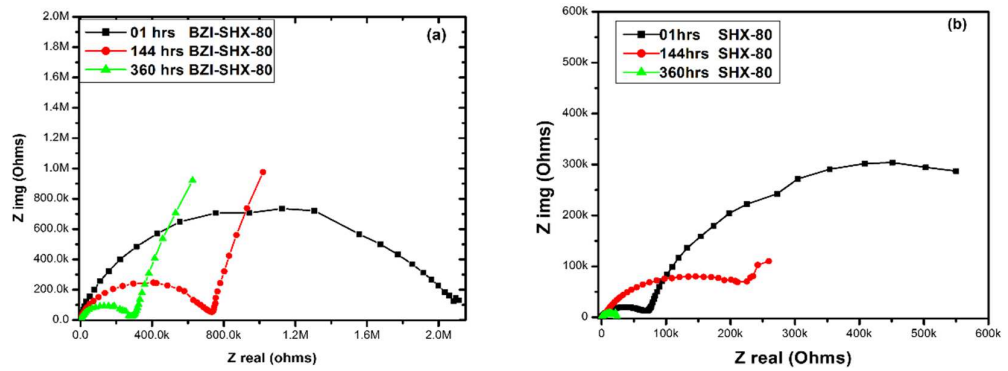


Figure 3.5, showing the Nyquist plot for (a) BZI-SHX-80 coating and (b) SHX-80 coating systems.

Figure 3.5 shows Nyquist plots for both (a) BZI-SHX-80 and (b) OA-SHX-80 coatings from 01 to 360 hr, respectively. These plots were used to obtain the equivalent circuits modelling fitting using ZSimpwin electrochemical impedance spectroscopy (EIS) data analysis software.

Tables 2 and 3 below demonstrate the fitted data for the SHX-80 and the BZI-SHX-80 coatings after various immersion times. The equivalent circuits were used to simulate the corrosion reaction on the surface of coated samples in 01 hr, 48hrs and 144 hrs, respectively. In these circuits, instead of using an ideal capacitor (C), a time-constant element (Q) was used to companies the current leakage in the capacitor and/or frequency dispersion effect of the alternating current signals [12]. The suggested equivalent circuits for each of the EIS plots after 144hrs were provided in the figure for both systems.

**Table 2** The fitted data obtained from EIS spectra for the BZI-SHX-80 sol-gel coating after various immersion times in 3.5 wt. % NaCl solution.

Element	Immersion time(hrs)		
	01	48	144
Circuit	R(Q(R(QR)))	R(Q(R(Q(RW))))	R(Q(R(Q(RW))))
R <sub>s</sub>	105	160	201
Q <sub>ct</sub>	1.471E-9	4.549E-9	9.148E-9
n	0.9626	0.887	0.8406
R <sub>ct</sub>	1.326E7	1.301E6	6.991E5
Q <sub>IL</sub>	3.453E-9	6.406E-8	9.016E-8
n	0.800	0.650	0.800
R <sub>IL</sub>	4.697E7	5.885E5	1.778E3
W	-	4.349E-8	7.044E-10

**Table 3** The fitted data obtained from EIS spectra for the SHX-80 sol-gel coating after various immersion times in 3.5 wt. % NaCl solution.

Element	Immersion time(hrs)		
	01	48	144
Circuit	R(Q(R(QR)))	R(Q(R(Q(R(QR))))	R(Q(R(Q(R(QR))))
R <sub>s</sub>	100	205	225
Q <sub>ct</sub>	1.079E-7	2.850E-7	4.771E-6
n	0.800	0.627	0.490
R <sub>ct</sub>	7.287E4	815	253
Q <sub>IL</sub>	4.933E-6	1.151E-6	3.912E-6
n	0.850	0.694	0.896
R <sub>IL</sub>	7.793E5	4.022E5	1.221E5
Q <sub>p</sub>	-	7.364E-5	4.835E-5
n	-	0.900	0.455
R <sub>p</sub>	-	1.369E6	1E20

1

3

4

5

6

7

8

9

10

11

12

13

14

15

16

17

18

19

The elements samples identifier used for the equivalent circuits were: solution resistance ( $R_s$ ), coating resistance ( $R_{ct}$ ), coating constant phase elements ( $Q_{ct}$ ), interfacial layer resistance ( $R_{iL}$ ), interfacial layer capacitance ( $Q_{iL}$ ), oxide layer (pitting) resistance ( $R_p$ ), oxide layer (pitting) capacitance ( $Q_p$ ) and Warburg-circuit element ( $W$ ) [15].

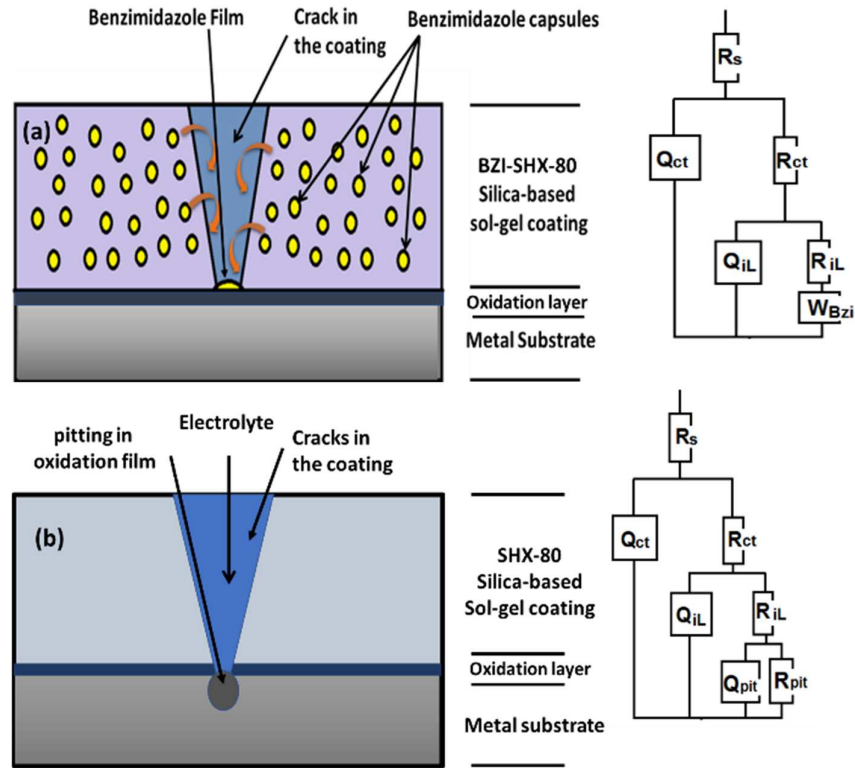


Figure 3.6 schematic drawing of the hybrid silica-based system (a) BZI-SHX-80 and (b) SHX-80 after 144 hr of immersion in 3.5% NaCl solution

### 3.5 Scanning Electron microscopy images after immersion

Figure 3.7 shows the surface morphology of the three samples, BZI-SHX-80, SHX-80, and bare alloy. It is clear that the bare sample is attacked by pitting corrosion after long immersion; as showed in figure 3.7 (c), in (b), the SHX-80 exhibited was susceptible to the development of microcracks when dried in open atmospheric conditions after long immersion. The cracks were observed around 1-6  $\mu\text{m}$  wide on the surface of the coating with some pitting under the coating. Exposure to the aluminium alloy substrate due to coating cracking can adversely affect the provided barrier corrosion protection, which has implications for wet/dry cycling is experienced. The BZI-SBX-80 coating showed excellent resistance to corrosion and cracks under similar circumstances, in figure 3.7 (a). The contact angle measurements showed that the ZBI-SHX-80 was more stable than the SHX-80, which may attributed prevent the diffusion in the coating system, in line with the benzimidazole self-healing inhibition properties.

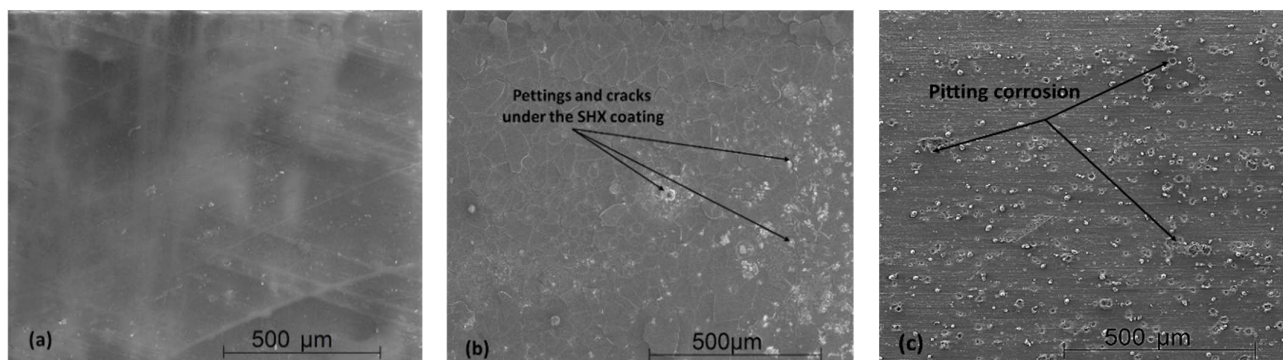


Figure 3.7 SEM surface images for (a) BZI-SHX-80 coating, (b) SHX-80 coating and (c) bare AA2024-t3 after 360hrs of immersion

#### 4. Conclusion

The base SHX Sol-gel formula can provide good barrier protection without the presence of any inhibitor. However, The protection can last for at least ten days in 3.5% NaCl solution before cracks and pitting appears visually on the coating surface. By encapsulating the benzimidazole in the silica-based sol-gel, it revealed excellent corrosion protection when combined with the hybrid silica-based sol-gel coatings formula, which can provide protection over two weeks without any failure sign. Adding benzimidazole as an inhibitor to the sol-gel matrix provides simulated active protection due to the high electronegativity active azole group. Also, it gains the highest impedance when compared to the original formal coating. Benzimidazole- sol-gel coating revealed an excellent resistance to post cracking after long immersion.

**Author Contributions:** Conceptualization, MM; methodology, MM, OL and NF; validation and testing MM; data analysis, MM., NF and OL; FTIR support, MM and DF; investigation, MM; resources, MM, OL and NF; writing—original draft preparation, MM; writing—review and editing, MM, OL and NF; project supervision, NF and OL; All authors have read and agreed to the published version of the manuscript.

**Funding:** This research was funded by the Libyan scholarship program as part of PhD project.

**Institutional Review Board Statement:** Not applicable

**Informed Consent Statement:** Not applicable.

**Data Availability Statement:** The data are not publicly available; The data files are stored on corresponding instruments and personal computers.

**Acknowledgements:** The authors would like to acknowledge the facilitating support by Sheffield Hallam University in Material and Engineering research institute (MERI) and also to the Libyan Scholarship Program for the financial support.

**Conflicts of Interest:** The authors declare no conflict of interest.

#### References

- [1] M. M. Antonijevic and M. B. Petrovic, "Copper corrosion inhibitors. A review," *Int. J. Electrochem. Sci.*, vol. 3, no. 1, pp. 1–28, 2008.
- [2] M. Antonijevic, S. Milic, M. Petrovic, M. Radovanovic, and A. Stamenkovic, "The Influence of pH and Chlorides on Electrochemical Behavior of Copper in the Presence of Benzotriazole," *Int. J. Electrochem. Sci*, vol. 4, no. July, pp. 962–979, 2009, [Online]. Available: [www.electrochemsci.org](http://www.electrochemsci.org).
- [3] J. B. Wright, "The Chemistry of the Benzimidazoles,," *Chem. Rev.*, vol. 48, no. 3, pp. 397–541, Jun. 1951, [Online]. Available: <https://pubs.acs.org/doi/abs/10.1021/cr60151a002>.



- [4] P. K. Gupta, "Herbicides and fungicides," in *Biomarkers in Toxicology*, Elsevier Inc., 2014, pp. 409–431. 1
- [5] E. Gutiérrez, J. A. Rodríguez, J. Cruz-Borbolla, J. G. Alvarado-Rodríguez, and P. Thangarasu, "Development of a predictive model for corrosion inhibition of carbon steel by imidazole and benzimidazole derivatives," *Corros. Sci.*, vol. 108, pp. 23–35, Jul. 2016, [Online]. Available: <http://dx.doi.org/10.1016/j.corsci.2016.02.036>. 2  
3  
4
- [6] I. B. Obot, A. Madhankumar, S. A. Umoren, and Z. M. Gasem, "Surface protection of mild steel using benzimidazole derivatives: Experimental and theoretical approach," *J. Adhes. Sci. Technol.*, vol. 29, no. 19, pp. 2130–2152, 2015, [Online]. Available: <http://dx.doi.org/10.1080/01694243.2015.1058544>. 5  
6  
7
- [7] F. Grillo, D. W. Tee, S. M. Francis, H. A. Früchtl, and N. V. Richardson, "Passivation of copper: Benzotriazole films on Cu(111)," *J. Phys. Chem. C*, vol. 118, no. 16, pp. 8667–8675, 2014. 8  
9
- [8] J. Colreavy, B. Duffy, R. Varma, Padinchare Covilakath, H. Hayden, and M. Oubaha, "Organosilane Coating Compositions and Use Thereof," Patent No: WO 2009/069111 A2, 2009. 10  
11
- [9] S. Vijaykumar, O. Prakash, S. Raghavan, K. Ramachandra, and D. Reddy, "Sol-gel coating compositions including corrosion inhibitor-encapsulated layered metal phosphates and related processes," Patent No: US 2018 / 0194949 A1, 2018. 12  
13
- [10] M. H. Mussa, Y. Rahaq, S. Takita, and N. Farmilo, "Study the Enhancement on Corrosion Protection by Adding PFDTES to Hybrid Sol-Gel on AA2024-T3 Alloy in 3.5% NaCl Solutions," *Albahit J. Appl. Sci.*, vol. 2, no. 1, pp. 61–68, Feb. 2021, Accessed: Feb. 05, 2021. [Online]. Available: <https://zenodo.org/record/4504652#.YNPIP9VKgps>. 14  
15  
16
- [11] ASTM International, "ASTM code B209 – 14 Standard Specification for Aluminum and Aluminum-Alloy Sheet and Plate," vol. 25. ASTM International, West Conshohocken, p. 16, 2016. 17  
18
- [12] W. S. Tait, *Electrochemical impedance spectroscopy fundamentals, an introduction to electrochemical corrosion testing for practicing engineers and scientists*. Racine, Wisconsin, USA: PairODocs Publications, 1994. 19  
20
- [13] S. Mohan, N. Sundaraganesan, and J. Mink, "FTIR and Raman studies on benzimidazole," *Spectrochim. Acta Part A Mol. Spectrosc.*, vol. 47, no. 8, pp. 1111–1115, 1991. 21  
22
- [14] D. Kumar *et al.*, "Development of durable self-cleaning coatings using organic-inorganic hybrid sol-gel method," *Appl. Surf. Sci.*, vol. 344, pp. 205–212, 2015, doi: 10.1016/j.apsusc.2015.03.105. 23  
24
- [15] A. Yabuki, H. Yamagami, and K. Noishiki, "Barrier and self-healing abilities of corrosion protective polymer coatings and metal powders for aluminum alloys," *Mater. Corros.*, vol. 58, no. 7, pp. 497–501, 2007. 25  
26  
27